

Sustainable Production of Selenium-Rich and Cadmium-Safe Rice by nZVI-Melatonin Synergy via Coordinated Plant-Microbe Regulation

Saiqa Menhas^{1,2,3}, Minjie Chen^{1,3}, Hui Jin^{1,3}, Jiang Xu^{1,3}, Saiyong Zhu², Muhammad Iqbal Zaman⁴, Jie Hou^{1,3*}, Daohui Lin^{1,2,3}

¹State Key Laboratory of Soil Pollution Control and Safety, College of Environmental and Resource Sciences, Zhejiang University, Hangzhou 310058, China.

²Zhejiang Ecological Civilization Academy, Anji 313300, P.R. China

³Zhejiang Provincial Key Laboratory of Organic Pollution Process and Control, College of Environmental and Resource Sciences, Zhejiang University, Hangzhou 310058, P.R. China

⁴Department of Chemistry, University of science and Technology, Bannu 28100, KP Pakistan

Correspondences *

Jie Hou (hou-jie@zju.edu.cn)

Table S1: The physio-chemical properties of contaminated paddy soil

Soil properties	Contaminated paddy soil
pH	5.42±0.08
N, g kg ⁻¹	3.08±0.12
P, g kg ⁻¹	2.15±0.13
K, g kg ⁻¹	12.39±1.17
Na, g kg ⁻¹	1.99±0.63
Ca, g kg ⁻¹	10.30±0.10
Mg, g kg ⁻¹	0.98±0.14
Mn, mg kg ⁻¹	181.42±27.13
TOC, %	2.32±0.27
Cd, mg kg ⁻¹	23.21±0.57
Cr, mg kg ⁻¹	127.02±3.40
Se, mg kg ⁻¹	3.73±0.16
Fe, g kg ⁻¹	20.90±0.35
sand, %	62
silt, %	18
clay, %	19
soil type	Sandy loam

Mean±SE. Note: TOC means total organic carbon content. Adapted from our previous studies ¹.

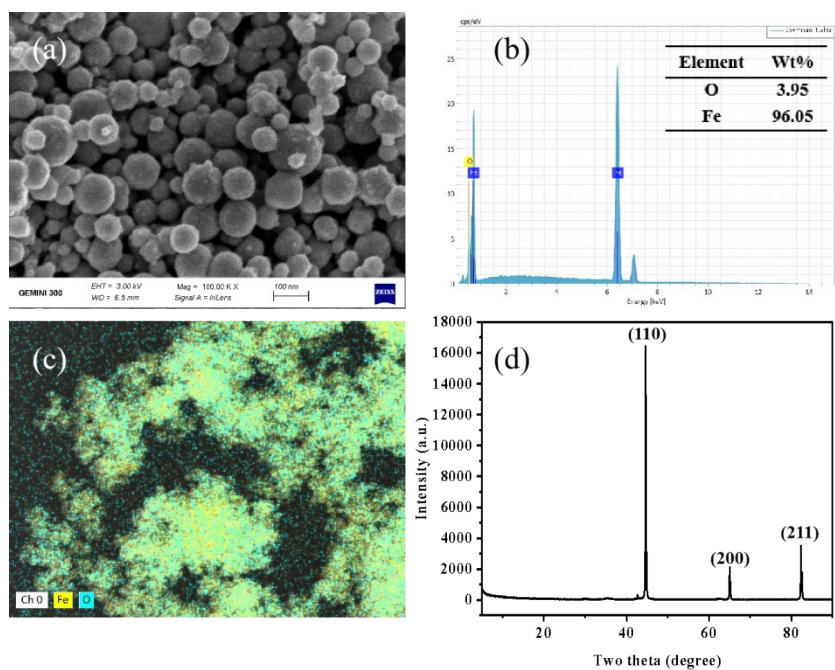


Figure S1 Characterizations of nZVI. (a) Scanning electron microscopy (SEM) showed that the nZVI was relatively spherical, with particle sizes ≤ 100 nm. (b) Energy dispersive X-ray spectroscopy (EDS) showed that oxygen and iron accounted for 3.95% and 96.05%, respectively, and (c) the two elements were uniformly distributed in the material. (d) The crystal structures of nZVI analyzed with X-ray diffraction (XRD). Adapted from our previous studies ².

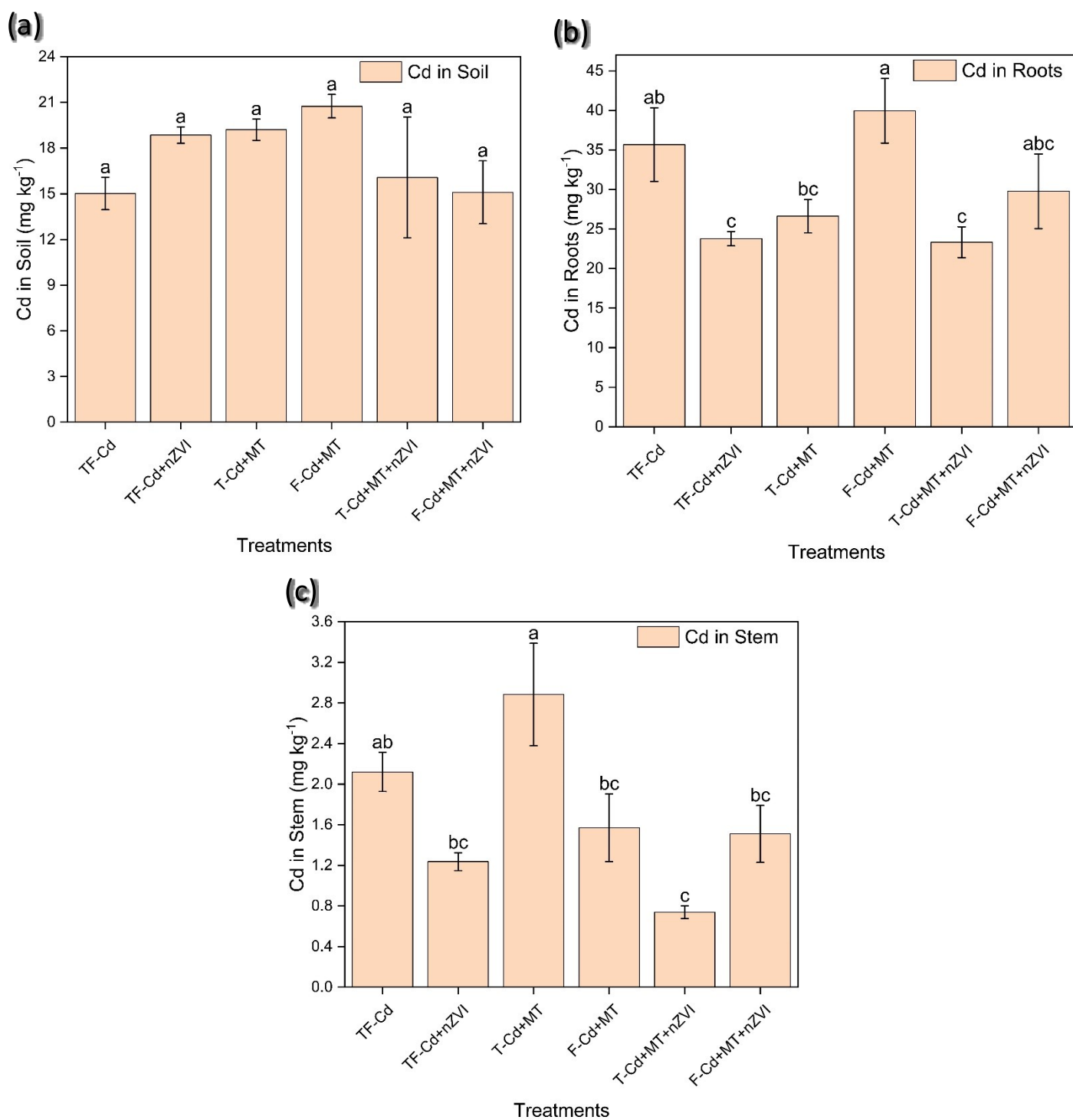


Figure S2: Effects of nZVI and MT on cadmium in (a) Soil, (b) Roots and (c) Stem across T and F developmental stages.

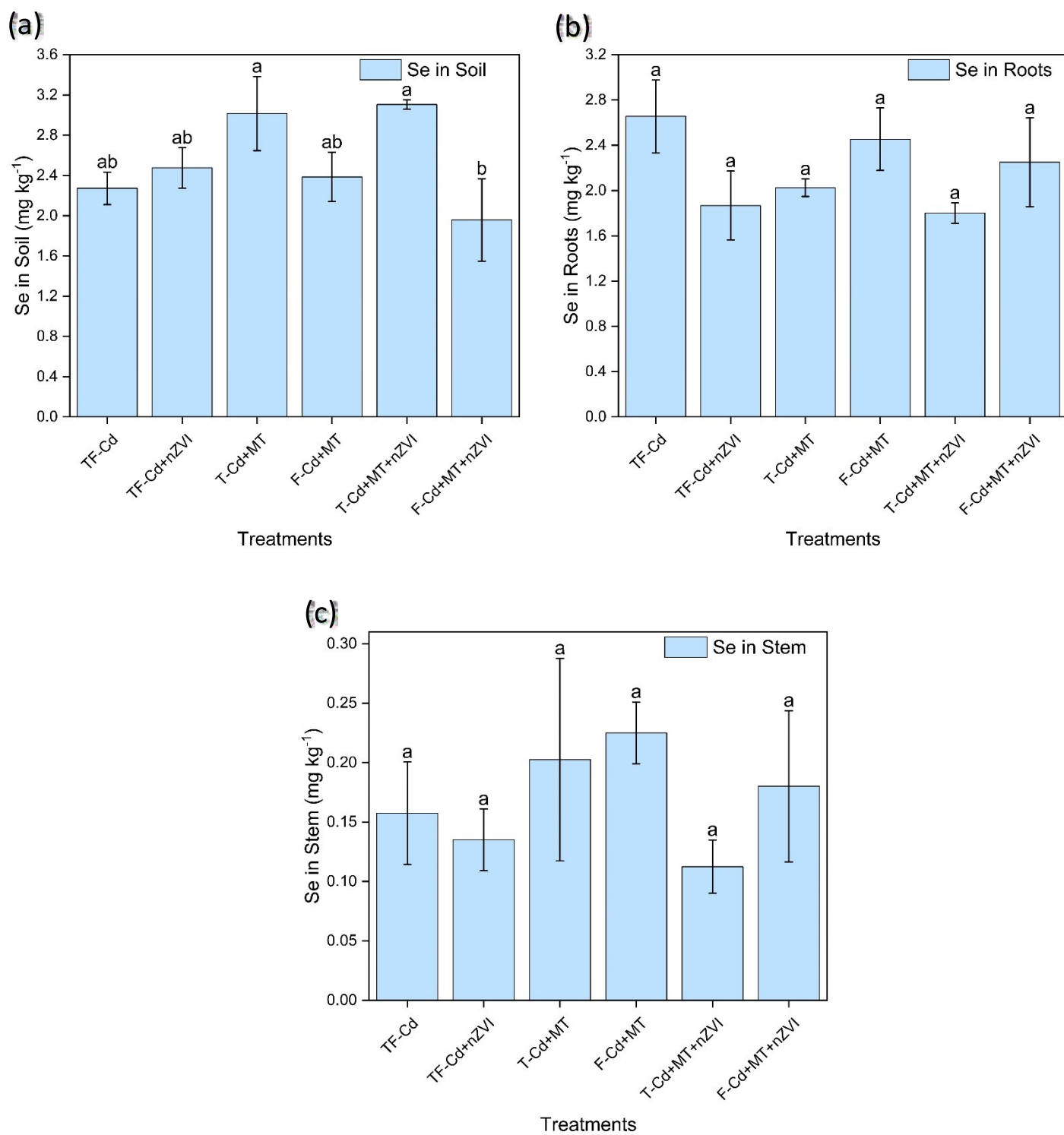


Figure S3: Effects of nZVI and MT on selenium in (a) Soil, (b) Roots and (c) Stem across T and F developmental stages.

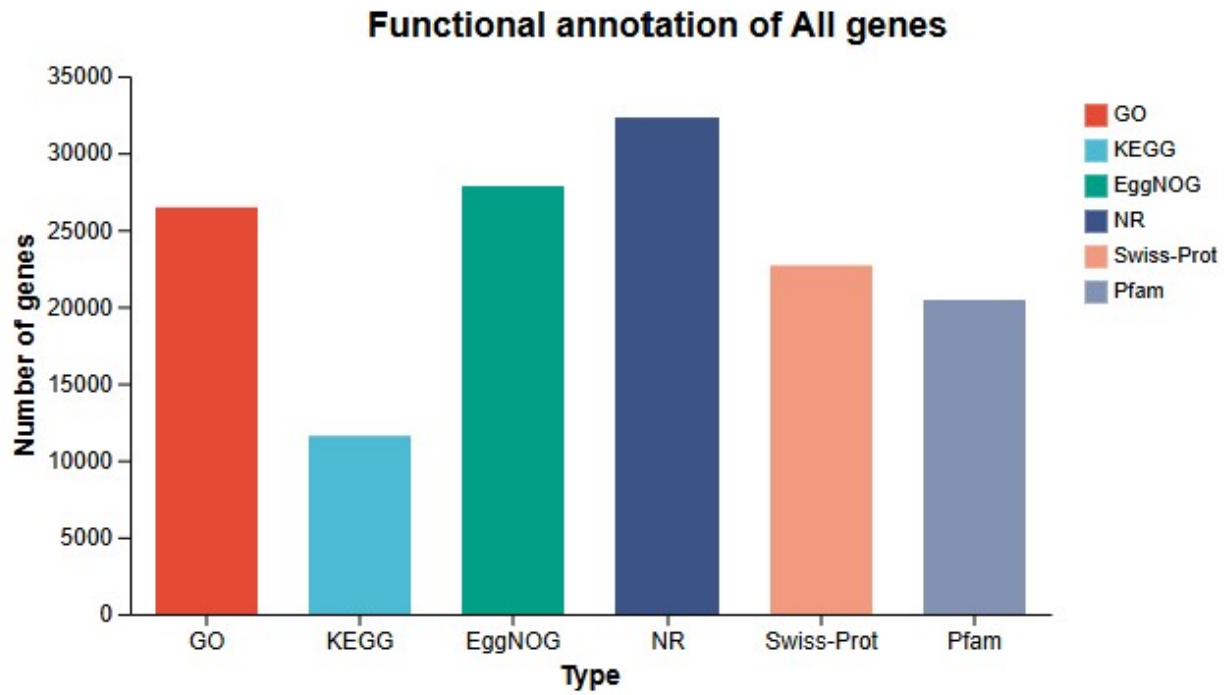


Figure S4: Functional annotation of all genes across six databases.

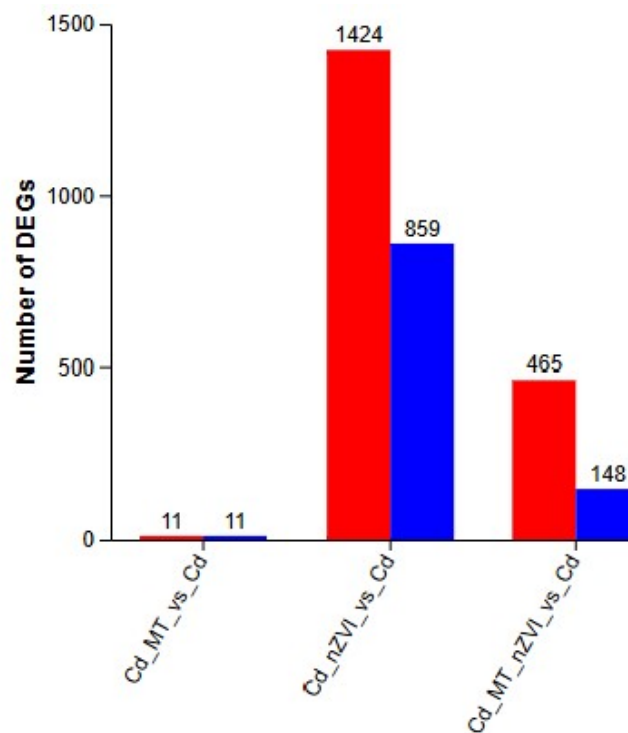


Figure S5: Distinct differentially expressed genes clusters across four treatments.

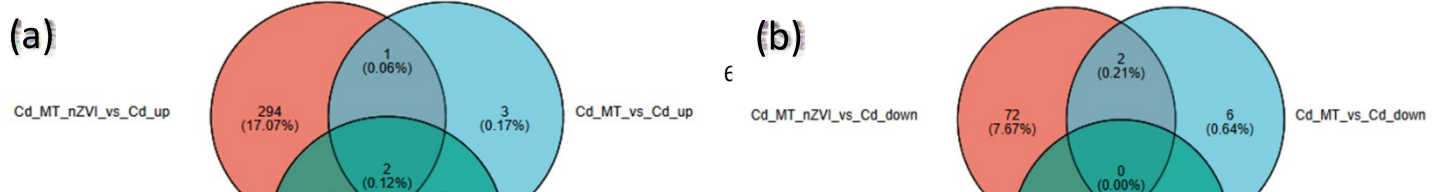


Figure S6: Venn diagrams of MT, nZVI, and their combinatorial treated groups.

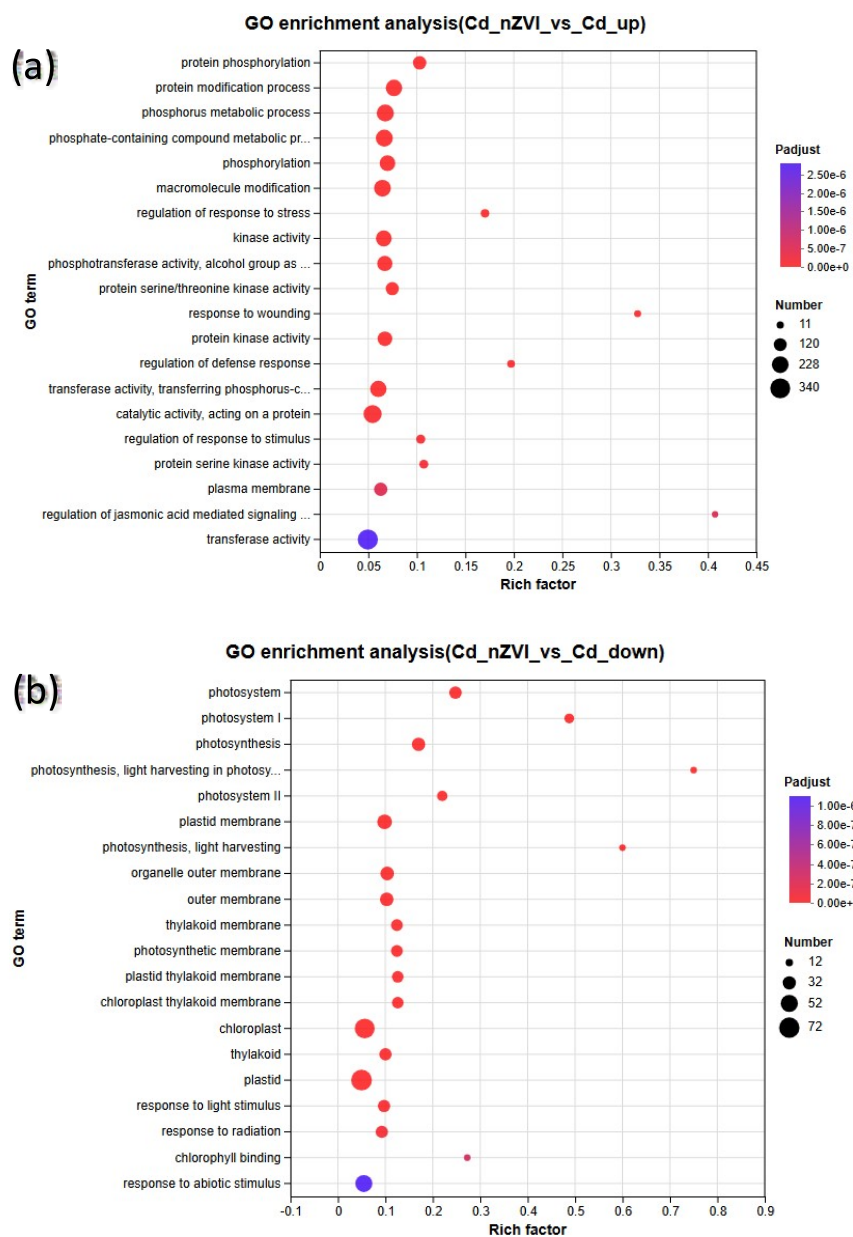
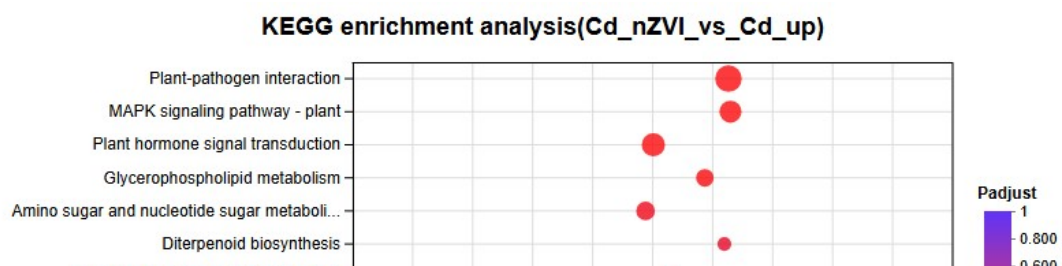


Figure S7: Effects of nZVI on (a) Up and (b) down Gene Ontology in the Cd vs. Cd-nZVI group.



(a)

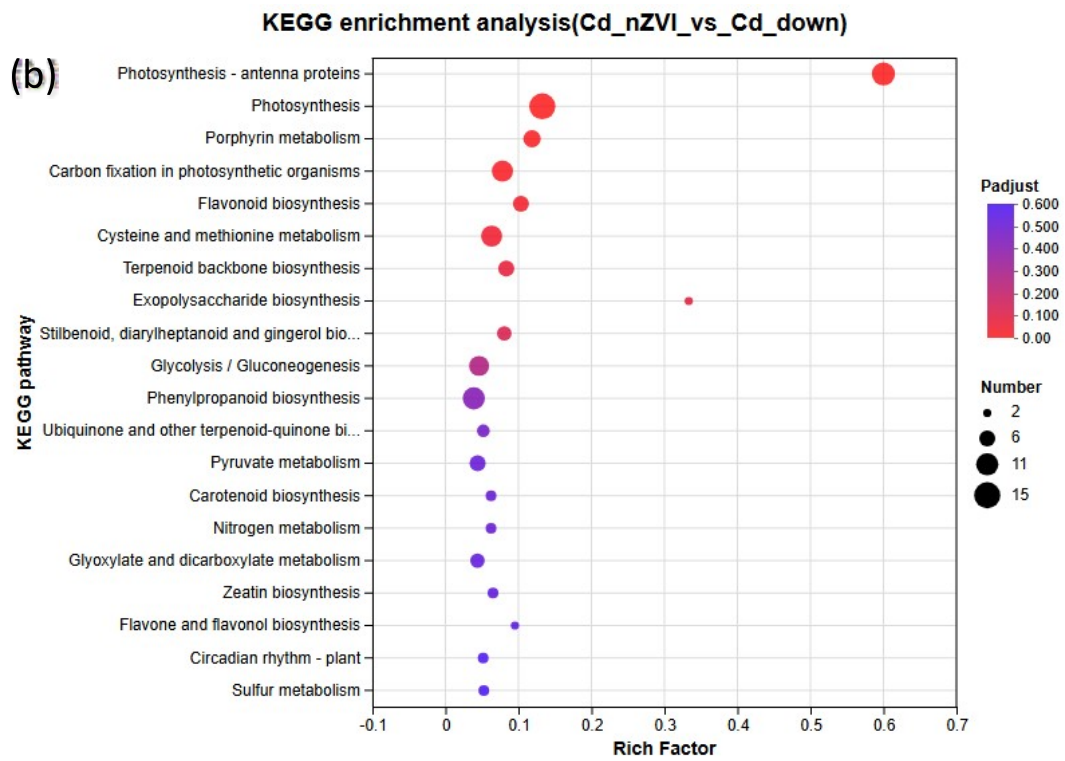


Figure S8: Effects of nZVI on (a) Up and (b) down Kyoto Encyclopedia of Genes and Genomes

enrichment analyses in the Cd vs. Cd-nZVI group.

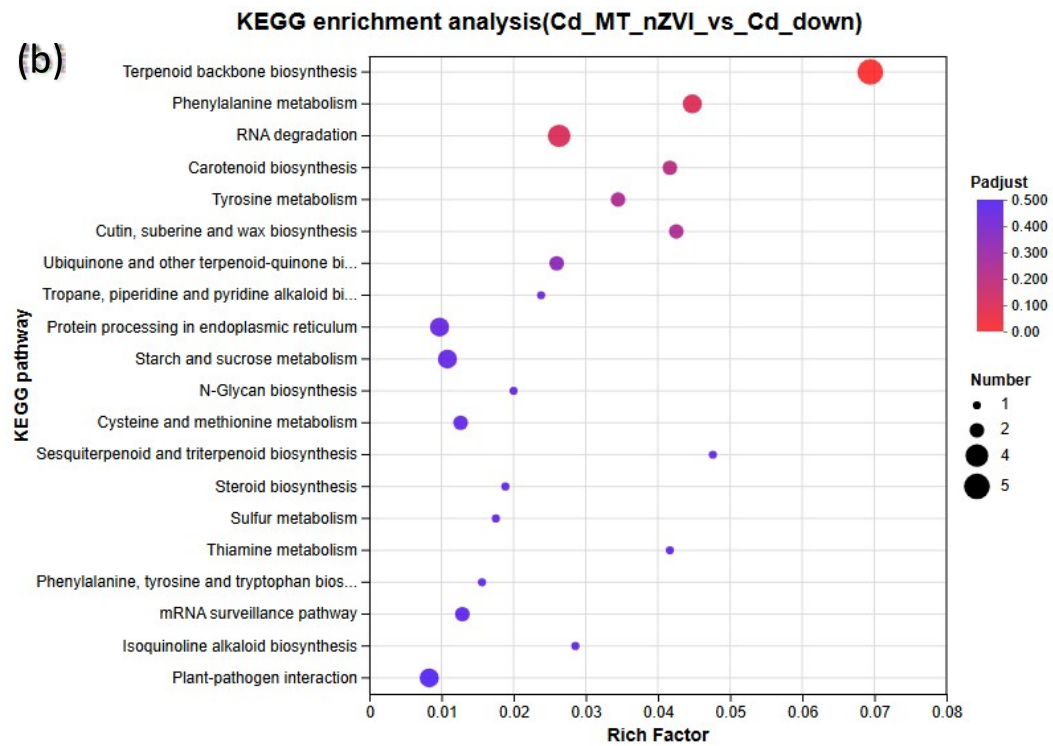
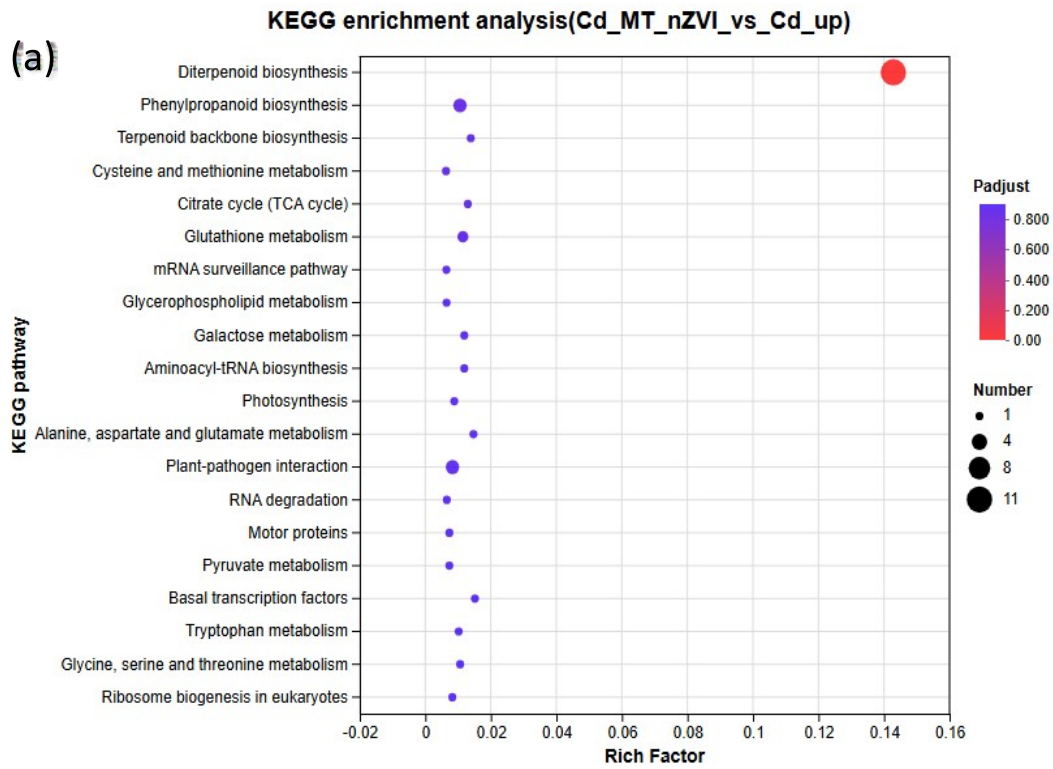


Figure S9: Effects of nZVI and MT on (a) Up and (b) down Kyoto Encyclopedia of Genes and Genomes enrichment analyses in the Cd vs. Cd-MT-nZVI group.

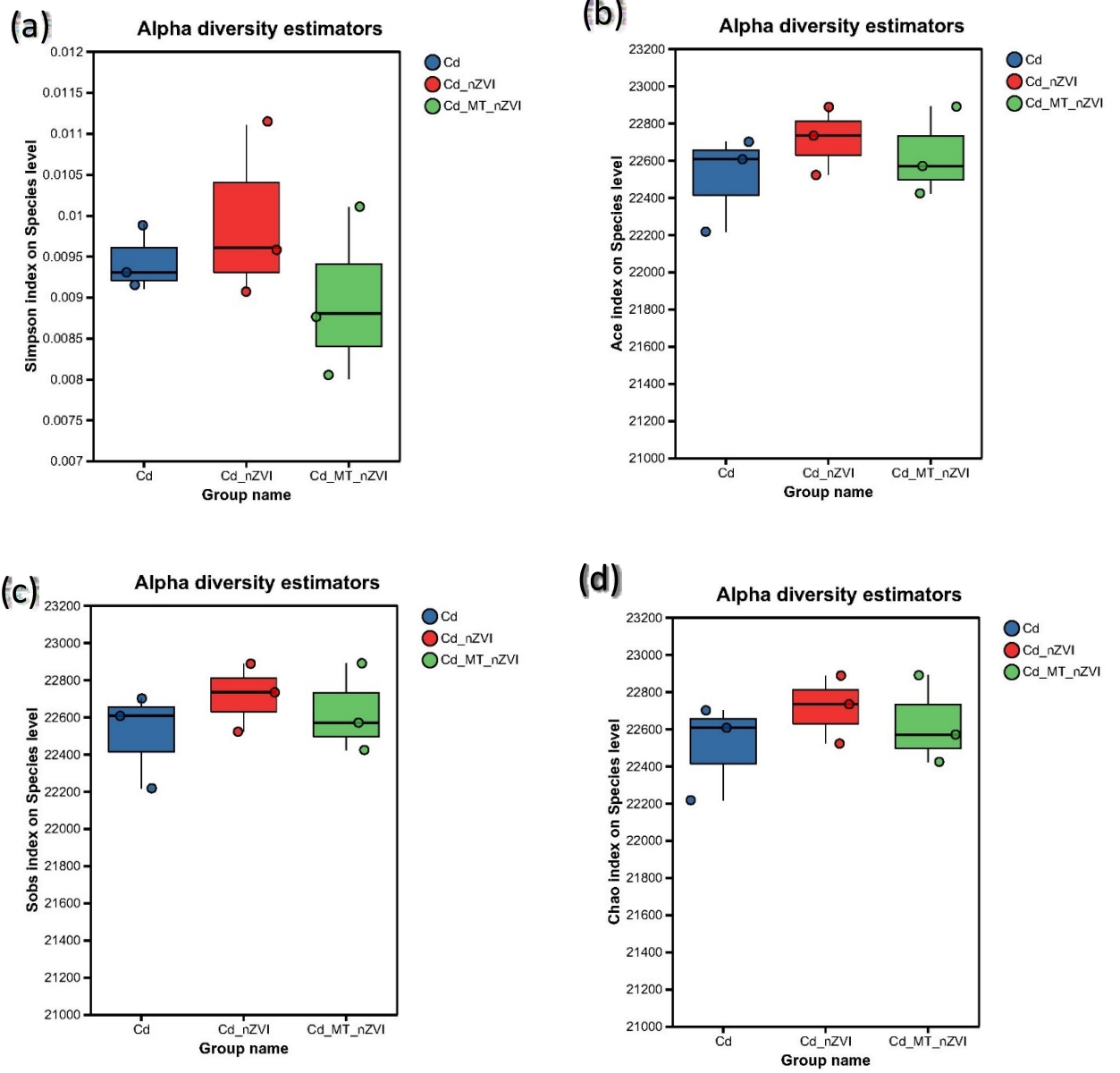


Figure S10: Microbial analysis. Alpha diversity (a) Simpson index, (b) Ace index, (c) Sobs index, and (d) Chao index on the species level across all treatments.

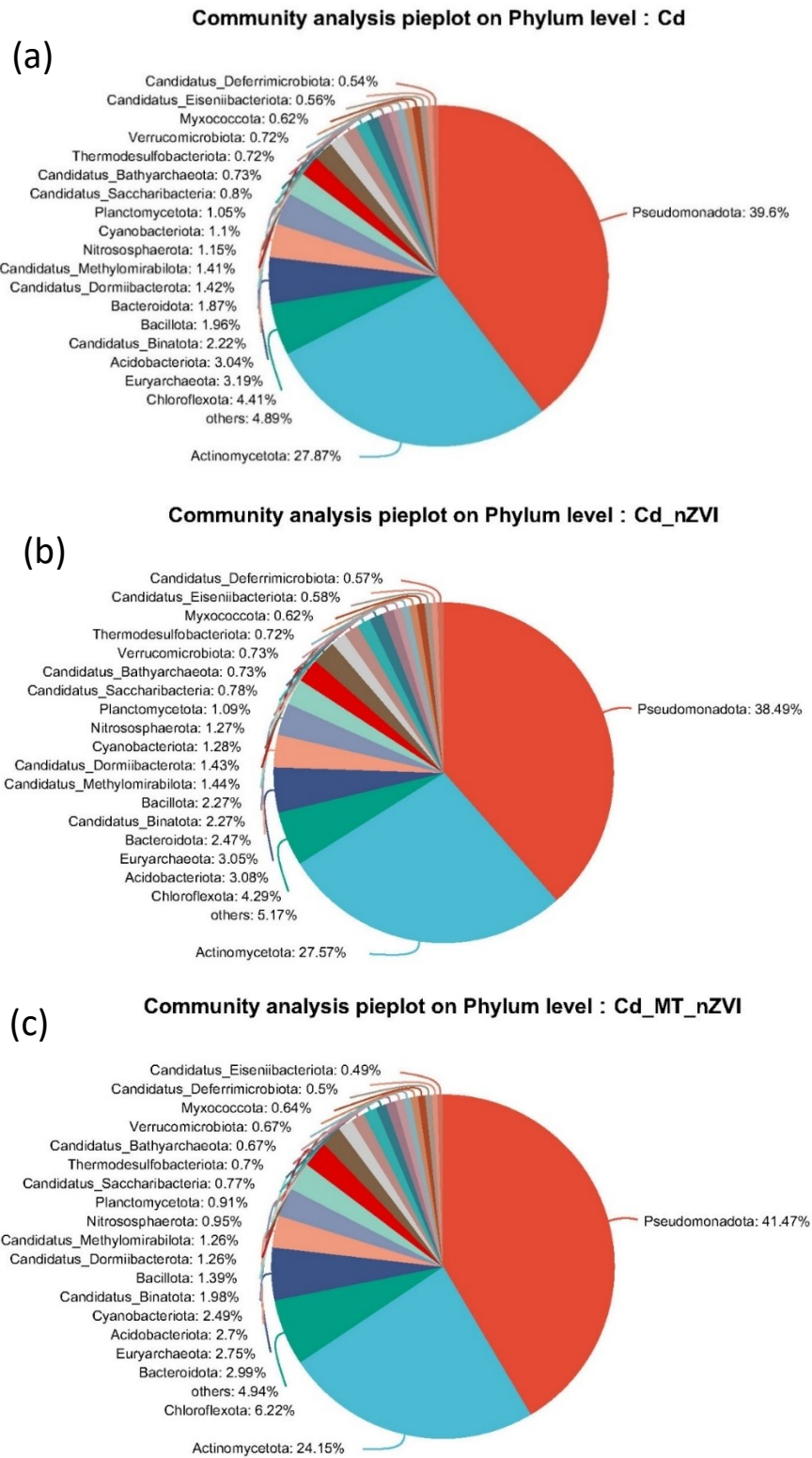


Figure S11: Effects of nZVI and MT on microbial community analysis in the (a) Cd, (b) Cd-nZVI, and (c) Cd-MT-nZVI groups on the phylum level.

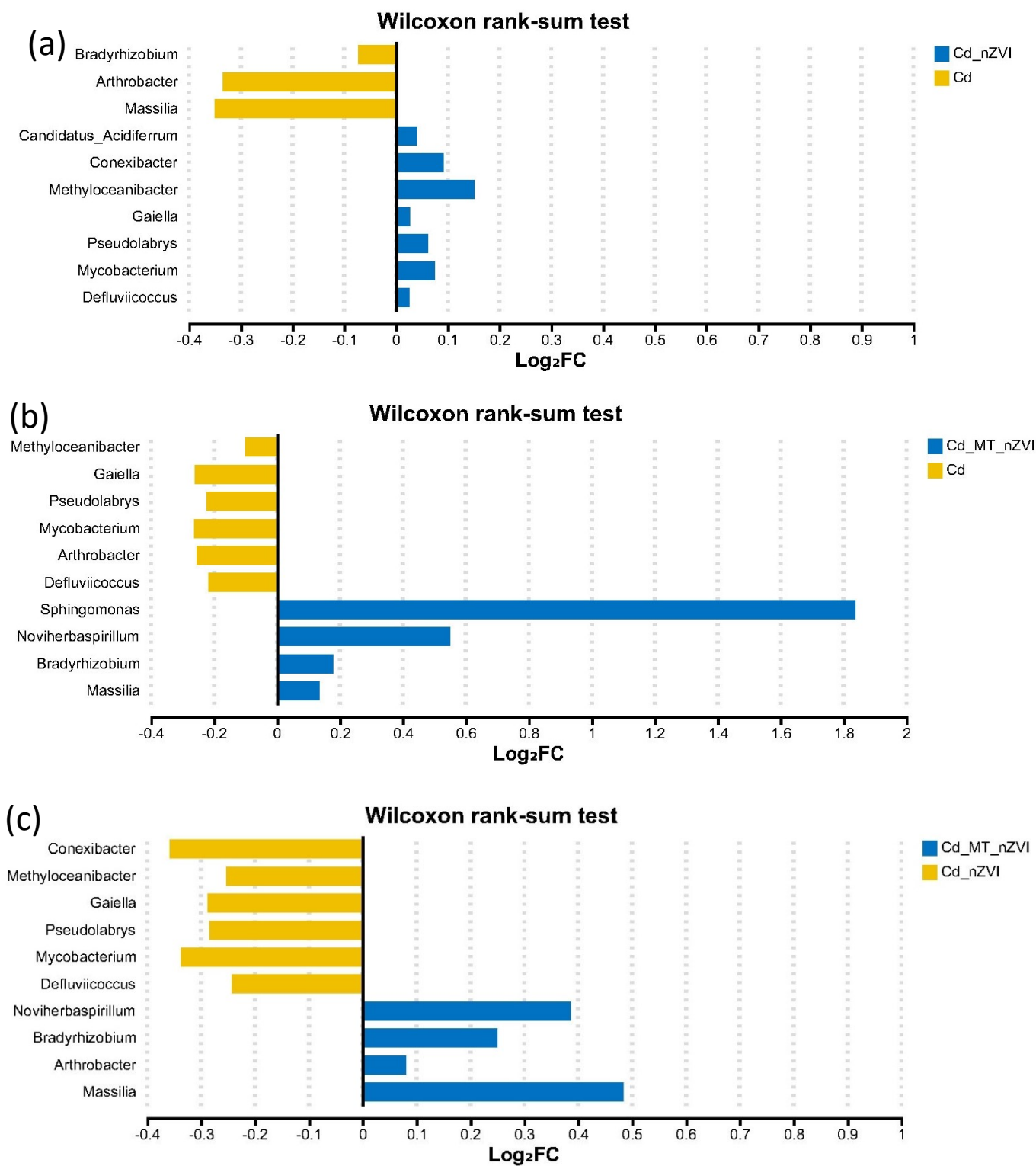


Figure S12: Effects of nZVI and MT on microbial community analysis, Wilcoxon rank-sum test in the (a) Cd, and Cd-nZVI, (b) Cd and Cd-MT-nZVI, (c) Cd-nZVI and Cd-MT-nZVI groups on genus level.

Results and discussion:

Supplementary Text S1:

Top 20 GOs and KEGG pathways in Cd vs Cd-nZVI group:

Comparative transcriptomic profiling of rice between Cd and Cd-nZVI treatments revealed a profound reprogramming of plant cellular processes, indicative of a strategic metabolic reallocation from primary productivity toward stress adaptation and defense mechanisms (Fig. S7 and S8). In the Cd-nZVI treatment group, differentially expressed genes (DEGs) were significantly enriched in biological processes associated with protein phosphorylation, phosphorus metabolic pathways, and jasmonic acid-mediated signaling pathways. These functional enrichments, coupled with dominant molecular functions linked to kinase and phosphotransferase activities, suggest the activation of intricate signal transduction networks. The pronounced representation of plasma membrane-associated components underscores the importance of early stress perception and membrane-associated signaling events in the nZVI-mediated response.

Consistent with gene ontology (GO) annotations, KEGG pathway analysis revealed significant upregulation of glycerophospholipid metabolism, MAPK signaling, plant hormone signal transduction, and plant-pathogen interaction pathways. These pathways are well-established mediators of abiotic stress tolerance, contributing to membrane integrity, hormonal cross-talk, and priming of defense responses. Conversely, downregulated DEGs in the Cd-nZVI comparison were predominantly associated with photosystem I and II components, thylakoid and plastid membranes, and chlorophyll-binding proteins. KEGG enrichment analysis further confirmed the suppression of photosynthesis, porphyrin metabolism, carbon fixation, and other light-harvesting processes in rice. This coordinated downregulation reflects a metabolic trade-off: energy and resources are redirected from photosynthetic apparatus maintenance toward stress mitigation and cellular protection. The concurrent repression of genes involved in circadian rhythm regulation supports a systemic reconfiguration of physiological timing, prioritizing survival over growth under combined Cd and nZVI exposure. These transcriptional dynamics support the dual hypothetical role of nZVI: (1) enhancing Cd immobilization and bioavailability reduction in the rhizosphere, and (2) potentiating intracellular stress signaling cascades while simultaneously reducing photosynthetic investment. Specifically, upregulation of glycerophospholipid metabolism likely contributes to membrane stabilization under heavy metal-induced oxidative stress, while activation of MAPK and phytohormone signaling pathways orchestrates downstream defense gene expression. In contrast, the downregulation of chlorophyll biosynthesis and thylakoid-related functions may minimize photooxidative damage by reducing light absorption and electron transport under suboptimal conditions, thereby conserving metabolic energy. While this resource reallocation enhances Cd tolerance and may facilitate improved Se uptake through altered ion homeostasis, it may also partially

explain the observed reduction in panicle number under nZVI treatment alone. This phenotype aligns with the well-documented phenomenon in which reproductive development is often sacrificed when defense pathways dominate metabolic allocation. These findings are consistent with prior studies demonstrating that nZVI influences root iron plaque formation, modulates nutrient dynamics, and elicits systemic stress responses in plants ³⁻⁷.

Top 20 GOs and KEGG pathways Cd vs Cd-MT-nZVI group:

Transcriptomic analysis of the Cd vs. Cd-MT-nZVI treatment comparison revealed that the combined amendment induces a coordinated and dynamic reprogramming of plant metabolism, simultaneously sustaining robust stress defense activation while restoring essential primary metabolic functions, most notably photosynthesis (Fig. 4f, g, and S9). DEGs upregulated under the co-treatment were significantly enriched in biological processes, including protein phosphorylation, cell surface receptor signaling, phosphorus-containing compound metabolism, and diterpenoid and terpenoid metabolic processes. The associated molecular functions, dominated by protein kinase, phosphotransferase, and carbohydrate/polysaccharide binding activities, suggest intensified signal transduction at the plasma membrane and subsequent activation of downstream regulatory and metabolic networks, particularly those governing secondary metabolism.

KEGG pathway enrichment analysis highlighted the induction of diterpenoid biosynthesis, a pathway known to produce phytoalexins and structurally diverse specialized metabolites implicated in heavy metal chelation and reactive oxygen species (ROS) scavenging ⁸⁻¹⁰. This supports the hypothesis that MT-nZVI co-treatment maintains a sustained, defense-oriented metabolic state. Furthermore, the concurrent upregulation of phenylpropanoid biosynthesis, glutathione metabolism, and glycerophospholipid metabolism indicates a multifaceted defense strategy integrating antioxidant biosynthesis, redox homeostasis, and membrane stabilization, thereby enhancing the cellular resilience of rice under Cd stress.

The co-treatment enhanced core metabolic pathways essential for energy and precursor supply. Upregulation of the citrate (TCA) cycle, cysteine and methionine metabolism, and alanine/aspartate/glutamate metabolism reflects a strategic reactivation of central carbon and amino acid metabolism. This metabolic reinforcement ensures a continuous flux of adenosine triphosphate (ATP), reducing equivalents, and biosynthetic intermediates, thereby supporting the energetic demands of prolonged stress responses. Additionally, activating plant-pathogen interaction and motor protein pathways implies engagement of biotic stress signaling modules and enhanced intracellular trafficking, potentially contributing to efficient allocation of defense components.

Conversely, downregulated DEGs were enriched in protein folding and refolding processes, isoprenoid biosynthesis, and chloroplast/plastid-localized functions. The suppression of chaperone-mediated folding and ATP-dependent protein folding machinery indicates a reduction in proteotoxic

stress, consistent with effective mitigation of Cd-induced protein damage. KEGG analysis further revealed significant downregulation of terpenoid backbone biosynthesis, carotenoid biosynthesis, and multiple alkaloid and steroid biosynthetic pathways. The apparent paradox, suppression of upstream terpenoid precursor synthesis alongside activation of downstream diterpenoid biosynthesis, likely reflects a feedback-driven attenuation mechanism, triggered upon sufficient accumulation of defensive end-products and the initiation of cellular homeostasis recovery¹⁰⁻¹².

A particularly salient feature of the MT-nZVI co-treatment is the reversal of photosynthetic suppression typically observed with nZVI application alone. The upregulation of photosynthesis-related pathways and the downregulation of chloroplast-localized protein misfolding and stress-related chaperones suggest that MT supplementation effectively restores chloroplast functionality. This alleviation of photosynthetic inhibition mitigates the energetic trade-offs imposed by nZVI-mediated stress prioritization, allowing for reallocating resources back toward growth and development. Given the central role of photosynthesis in biomass accumulation and yield formation, this restoration is critical for maintaining plant productivity under metal stress⁸⁻¹⁰. Taken together, these transcriptional dynamics indicate that the MT-nZVI co-treatment orchestrates a dual metabolic strategy: (1) the sustained activation of defense pathways via diterpenoid and phenylpropanoid biosynthesis, antioxidant systems, and stress-responsive signaling; and (2) the reactivation of primary metabolism, particularly photosynthesis and energy metabolism, to support physiological recovery and growth. This integrative molecular reconfiguration provides a mechanistic basis for the improved physiological performance, enhanced stress tolerance, reduced oxidative damage, and higher yield potential observed in plants exposed to Cd-contaminated environments when treated with the combined MT-nZVI amendment.

Supplementary Text S2:

Transcriptomic analyses of nZVI and nZVI+MT treatments reveal a convergent metabolic reprogramming that channels plant physiology toward specialized defense deployment, enhanced redox regulation, and recalibrated growth, providing a coherent molecular framework for the dual modulation of Cd tolerance and Se acquisition (Table S4, S6, and S8 in Appendix B). A core conserved response across both treatment centers on the plastidial methylerythritol phosphate (MEP)-derived diterpenoid biosynthesis pathway, with coordinated upregulation of key biosynthetic genes: *OsDXS*, *OsCPS2/4*, *OsKSL10*, *Oscyp71Z6*, and *OsSDR110C-MS2*. These enzymes direct isoprenoid precursors through cyclization and oxidative tailoring to generate phytoalexins such as momilactones, which are well-documented for their metal-chelating properties and ROS-scavenging capacity. This transcriptional signature reflects a sustained state of chemical immunity under heavy metal stress. It is reinforced by concurrent enrichment in kinase- and receptor-mediated signaling pathways, indicating membrane-proximal stress perception that directly activates secondary metabolic circuits,

particularly the diterpenoid defense axis^{9, 13, 14}.

Concomitant upregulation of *OsPAL2*, a pivotal gene in phenylpropanoid metabolism, diverts flux toward synthesizing phenolics and flavonoids, reinforcing cell wall integrity and mitigating oxidative damage. This complements diterpenoid-based defenses, collectively expanding the plant's antioxidant reservoir and fortifying structural barriers. Additionally, induction of the auxin-responsive *OsSAUR11* suggests hormonal crosstalk that recalibrates growth under stress, potentially through modulation of root architecture, exudate composition, and rhizosphere interactions. These adjustments may promote Cd immobilization in the rhizosphere while enhancing Se bioavailability at the soil-root interface^{9, 15-17}, reflecting not a passive growth penalty but an active optimization of defense-growth trade-offs.

Beyond secondary metabolism, primary metabolic and membrane biophysical adaptations further stabilize stress resilience. Upregulation of *GPAT* (glycerol-3-phosphate acyltransferase) implies cutin and membrane lipid remodeling, reinforcing apoplastic and plasma membrane integrity while modulating fluidity to preserve signaling fidelity. Concurrently, induction of *pckA* (phosphoenolpyruvate carboxykinase) indicates flexible carbon routing, balancing gluconeogenic flux and anaplerotic replenishment of TCA cycle intermediates to sustain defense biosynthesis without depleting energy reserves^{9, 18}. The peroxisomal glycolate oxidase *GLO6* is also induced, enhancing H₂O₂ catabolism in coordination with plastidic and cytosolic antioxidant systems (e.g., glutathione and ascorbate pathways), thereby tightening redox homeostasis during Cd exposure¹⁵.

A defining feature of the nZVI+MT co-treatment is the preservation and recovery of photosynthetic capacity, even amid sustained defense activation. This is evidenced by the attenuation of chloroplast protein misfolding signatures (reduced chaperone/folding demand) alongside the reactivation of photosynthesis-related pathways. This transcriptional profile supports the restoration of chloroplast function and explains the maintenance of growth and yield potential under stress, consistent with MT-mediated alleviation of proteotoxic stress and protection of photosynthetic apparatus integrity⁸⁻¹⁰. Notably, the apparent paradox of downregulated terpenoid backbone biosynthesis genes alongside upregulated downstream diterpenoid branches is congruent with a feedback attenuation mechanism. Once defensive end-products accumulate and cellular homeostasis begins to recover, upstream precursor synthesis is downregulated to prevent metabolic overcommitment and futile cycling, while branch-specific enzymes continue to sustain targeted phytoalexin production¹⁰⁻¹².

The shared set of 158 DEGs regulated by both nZVI and nZVI+MT delineates a conserved core regulatory module encompassing: (i) diterpenoids and phenylpropanoids biosynthesis, (ii) receptor/kinase signaling, (iii) lipid and membrane remodeling, (iv) carbon and energy flexibility, and (v) peroxisomal ROS control. This transcriptional network constitutes a molecular scaffold that

integrates Cd detoxification, via chelation, sequestration, and transporter-mediated compartmentalization, with enhanced Se uptake and micronutrient acquisition^{9, 13, 14}. The co-treatment thus enables the coexistence of high defense readiness and preserved photosynthetic function, a critical balance for sustaining productivity in contaminated environments^{8, 10}.

Convergent downregulation further clarifies a strategic metabolic reprioritization under combined Cd stress and remediation (Table S5, S7, and S9 in Appendix B). Suppression of *CABIR*, a chlorophyll *a/b*-binding protein in photosystem I (PSI), suggests a deliberate reduction in light-harvesting antenna size, minimizing excess excitation and photodamage under stress while redirecting resources to defense biosynthesis. Reduced expression of *HSP90B* and other chaperones indicates reduced proteotoxic burden, consistent with effective mitigation of Cd-induced protein misfolding. Diminished *SSIIB* (starch synthase IIIb) redirects carbon flux from starch storage toward more labile energy pools and defense metabolites. Similarly, suppression of *FDPS*, *IPI*, and *OsHDR* throttles isoprenoid precursor generation, aligning flux with downstream demand. Reduced expression of *SRD5A3* and *OsSTA246* indicates selective deprioritization of lipid and polysaccharide processing, while downregulation of *MDH2* (malate dehydrogenase) and splicing factors (*SRSF10/FUSIP1*) suggests a temporary scaling back of TCA cycle throughput and mRNA processing, energy-intensive processes curtailed during adaptive restructuring¹⁹.

These transcriptomic shifts align with observed physiological outcomes of reduced oxidative damage, improved growth performance, and higher yield stability in nZVI+MT-treated plants. Critically, the effects are not merely additive but synergistic, integrating stress signaling, antioxidant biosynthesis, ion transport, hormonal regulation, and systemic metabolic reconfiguration into a cohesive, self-reinforcing defense strategy²⁰⁻²³. This synergy enables: (i) detoxification via chelation and vacuolar sequestration, (ii) tolerance through stress-protective proteins and osmoprotectants, and (iii) improved nutritional status via enhanced uptake of Se and other beneficial elements; all while preserving sufficient photosynthetic capacity to sustain growth and yield²²⁻²⁶. Furthermore, dynamic interactions with the rhizosphere microbiome likely amplify this response. Altered root exudation patterns and immune signaling under nZVI+MT may foster beneficial microbial consortia that enhance nutrient mobilization (particularly Se), suppress phytopathogens, and prime systemic acquired resistance, reinforcing plant resilience through plant-microbe feedback loops.

Collectively, these findings support a systems-level model in which nZVI establishes a defense-centric metabolic state anchored in diterpenoid and phenylpropanoid pathways, membrane remodeling, and redox tightening, while MT co-treatment restores chloroplast functionality and rebalances energy allocation. The conserved core of 158 integrates Cd detoxification and Se acquisition, stabilizing growth under stress. Thus, nZVI+MT catalyzes a resilient, self-reinforcing plant-microbe alliance, optimized for productivity in heavy metal-impacted environments.

References:

1. S. Menhas, M. Chen, H. Jin, J. Xu, S. Zhu and D. Lin, Plant growth stage and melatonin concentration dependency together drive the metal-nutrient dynamics of rice in paddy soil, *Int J Phytoremediation*, 2025, **27**, 958-971.
2. G. Su, B. Chen, X. Wu, J. Xu, K. Yang and D. Lin, nZVI decreases N₂O emission from pesticide-contaminated paddy soil, *Sci Total Environ*, 2023, **892**, 164613.
3. Q. Bao, Y. Bao, J. Shi and Y. Sun, Nano zero-valent iron and melatonin synergistically alters uptake and translocation of Cd and As in soil-rice system and mechanism in soil chemistry and microbiology, *Environ Int*, 2024, **185**, 108550.
4. K. Li, J. Li, F. Qin, H. Dong, W. Wang, H. Luo, D. Qin, C. Zhang and H. Tan, Nano zero valent iron in the 21st century: A data-driven visualization and analysis of research topics and trends, *Journal of Cleaner Production*, 2023, **415**.
5. J. Wang, Z. Fang, W. Cheng, X. Yan, P. E. Tsang and D. Zhao, Higher concentrations of nanoscale zero-valent iron (nZVI) in soil induced rice chlorosis due to inhibited active iron transportation, *Environ Pollut*, 2016, **210**, 338-345.
6. T. Bao, M. M. Dantie, C. Y. Wang, C. L. Li, Z. Chen, K. Cho, W. Wei, P. Yuan, R. L. Frost and B. J. Ni, Iron-containing nanominerals for sustainable phosphate management: A comprehensive review and future perspectives, *Sci Total Environ*, 2024, **926**, 172025.
7. D. Hou, X. Cui, M. Liu, H. Qie, Y. Tang, R. Xu, P. Zhao, W. Leng, N. Luo, H. Luo, A. Lin, W. Wei, W. Yang and T. Zheng, The effects of iron-based nanomaterials (Fe NMs) on plants under stressful environments: Machine learning-assisted meta-analysis, *J Environ Manage*, 2024, **354**, 120406.
8. A. K. Kathirvel, K. M. Karuppasami, V. Dhashnamurthi, G. Vellingiri, R. Muthurajan, A. Venugopal, A. Kuppusamy and S. Alagarsamy, Enhancement of grain yield in rice under combined drought and high-temperature stress conditions by maintaining photosynthesis through antioxidant enzyme activities by melatonin, *Plant Physiology Reports*, 2024, **29**, 262-277.
9. S. Menhas, X. Yang, K. Hayat, J. Bundschuh, X. Chen, N. Hui, D. Zhang, S. Chu, Y. Zhou, E. F. Ali, M. Shahid, J. Rinklebe, S. S. Lee, S. M. Shaheen and P. Zhou, Pleiotropic melatonin-mediated responses on growth and cadmium phytoextraction of *Brassica napus*: A bioecological trial for enhancing phytoremediation of soil cadmium, *J Hazard Mater*, 2023, **457**, 131862.

10. C. W. Qiu, M. Richmond, Y. Ma, S. Zhang, W. Liu, X. Feng, I. M. Ahmed and F. Wu, Melatonin enhances cadmium tolerance in rice via long non-coding RNA-mediated modulation of cell wall and photosynthesis, *J Hazard Mater*, 2024, **465**, 133251.
11. Y. Q. Gao, R. Guo, H. Y. Wang, J. Y. Sun, C. Z. Chen, D. Hu, C. W. Zhong, M. M. Jiang, R. F. Shen, X. F. Zhu and J. Huang, Melatonin Increases Root Cell Wall Phosphorus Reutilization via an NO Dependent Pathway in Rice (*Oryza sativa*), *J Pineal Res*, 2024, **76**, e12995.
12. J. Huang, H. K. Jing, Y. Zhang, S. Y. Chen, H. Y. Wang, Y. Cao, Z. Zhang, Y. H. Lu, Q. S. Zheng, R. F. Shen and X. F. Zhu, Melatonin reduces cadmium accumulation via mediating the nitric oxide accumulation and increasing the cell wall fixation capacity of cadmium in rice, *J Hazard Mater*, 2023, **445**, 130529.
13. S. Zhao, Q. Zhang, W. Xiao, D. Chen, J. Hu, N. Gao, M. Huang and X. Ye, Comparison of Transcriptome Differences between Two Rice Cultivars Differing in Cadmium Translocation from Spike-Neck to Grain, *Int J Mol Sci*, 2024, **25**.
14. S. Zhu, S. Sun, W. Zhao, X. Yang, H. Mao, L. Sheng and Z. Chen, Utilizing transcriptomics and proteomics to unravel key genes and proteins of *Oryza sativa* seedlings mediated by selenium in response to cadmium stress, *BMC Plant Biol*, 2024, **24**, 360.
15. Y. Song, B. Wang, D. Qiu, Z. Xie, S. Dai, C. Li, S. Xu, Y. Zheng, S. Li and M. Jiang, Melatonin enhances metallic oxide nanoparticle stress tolerance in rice via inducing tetrapyrrole biosynthesis and amino acid metabolism, *Environmental Science: Nano*, 2021, **8**, 2310-2323.
16. S. Zhao, Q. Zhang, W. Xiao, D. Chen, J. Hu, N. Gao, M. Huang and X. Ye, Comparative transcriptomic analysis reveals the important process in two rice cultivars with differences in cadmium accumulation, *Ecotoxicol Environ Saf*, 2023, **252**, 114629.
17. S. Zhao, Q. Zhang, W. Xiao, D. Chen, J. Hu, N. Gao, M. Huang and X. Ye, Comparative transcriptome analysis reveals key genes and coordinated mechanisms in two rice cultivars differing in cadmium accumulation, *Chemosphere*, 2023, **338**, 139489.
18. R. Munir, M. U. Yasin, M. Afzal, M. Jan, S. Muhammad, N. Jan, C. Nana, F. Munir, H. Iqbal, F. Tawab and Y. Gan, Melatonin alleviated cadmium accumulation and toxicity by modulating phytohormonal balance and antioxidant metabolism in rice, *Chemosphere*, 2024, **346**, 140590.
19. Y. Yu, Q. Wang, Y. Wan, Q. Huang and H. Li, Transcriptome analysis reveals different mechanisms of selenite and selenate regulation of cadmium translocation in *Brassica rapa*, *J Hazard Mater*, 2023, **452**, 131218.

20. J. Wang, Y. Lu, S. Xing, J. Yang, L. Liu, K. Huang, D. Liang, H. Xia, X. Zhang, X. Lv and L. Lin, Transcriptome analysis reveals the promoting effects of exogenous melatonin on the selenium uptake in grape under selenium stress, *Front Plant Sci*, 2024, **15**, 1447451.
21. R. Jan, S. Asif, S. Asaf, Lubna, X. X. Du, J. R. Park, K. Nari, D. Bhatta, I. J. Lee and K. M. Kim, Melatonin alleviates arsenic (As) toxicity in rice plants via modulating antioxidant defense system and secondary metabolites and reducing oxidative stress, *Environ Pollut*, 2023, **318**, 120868.
22. Z. Liu, H. Sun, Y. Li, Q. Bao and Y. Huang, Metabolic regulation mechanism of melatonin for reducing cadmium accumulation and improving quality in rice, *Food Chem*, 2024, **455**, 139857.
23. C. Zhou, P. Miao, Q. Dong, D. Li and C. Pan, Multiomics Explore the Detoxification Mechanism of Nanoselenium and Melatonin on Bensulfuron Methyl in Wheat Plants, *J Agric Food Chem*, 2024, **72**, 3958-3972.
24. T. Guha, S. Barman, A. Mukherjee and R. Kundu, Nano-scale zero valent iron modulates Fe/Cd transporters and immobilizes soil Cd for production of Cd free rice, *Chemosphere*, 2020, **260**, 127533.
25. K. Wang, H. Yu, X. Zhang, D. Ye, H. Huang, Y. Wang, Z. Zheng and T. Li, A transcriptomic view of cadmium retention in roots of cadmium-safe rice line (*Oryza sativa* L.), *J Hazard Mater*, 2021, **418**, 126379.
26. H. Yang, H. Yu, S. Wang, H. Huang, D. Ye, X. Zhang, T. Liu, Y. Wang, Z. Zheng and T. Li, Comparative transcriptomics reveals the key pathways and genes of cadmium accumulation in the high cadmium-accumulating rice (*Oryza Sativa* L.) line, *Environ Int*, 2024, **193**, 109113.